

Article

# Wind Speed Forecasting Based on EMD and GRNN Optimized by FOA

Dongxiao Niu <sup>1</sup>, Yi Liang <sup>1,\*</sup> and Wei-Chiang Hong <sup>2</sup> 

<sup>1</sup> School of Economics and Management, North China Electric Power University, Beijing 102206, China; ndx@ncepu.edu.cn

<sup>2</sup> Department of Information Management, Oriental Institute of Technology, New Taipei 220, Taiwan; samuelsonhong@gmail.com

\* Correspondence: louisliang@ncepu.edu.cn; Tel.: +86-010-61773079

Received: 13 November 2017; Accepted: 28 November 2017; Published: 1 December 2017

**Abstract:** As a kind of clean and renewable energy, wind power is winning more and more attention across the world. Regarding wind power utilization, safety is a core concern and such concern has led to many studies on predicting wind speed. To obtain a more accurate prediction of the wind speed, this paper adopts a new hybrid forecasting model, combining empirical mode decomposition (EMD) and the general regression neural network (GRNN) optimized by the fruit fly optimization algorithm (FOA). In this new model, the original wind speed series are first decomposed into a collection of intrinsic mode functions (IMFs) and a residue. Next, the inherent relationship (partial correlation) of the datasets is analyzed, and the results are then used to select the input for the forecasting model. Finally, the GRNN with the FOA to optimize the smoothing factor is used to predict each sub-series. The mean absolute percentage error of the forecasting results in two cases are respectively 8.95% and 9.87%, suggesting that the hybrid approach outperforms the compared models, which provides guidance for future wind speed forecasting.

**Keywords:** wind speed forecasting; empirical mode decomposition; general regression neural network; fruit fly optimization algorithm

## 1. Introduction

Wind power, as a type of sustainable and clean energy, is one of the most widely used, technologically mature, and commercially produced renewable sources [1,2]. According to the Global Wind Energy Council (GWEC), the cumulative wind generating installed capacity has reached 486,790 MW at the end of 2016 with the share of 34.7% donated by China [3]. The goal that grid-connected wind power installed capacity should reach 200 GW by 2020 [4] indicates that, during the “13th Five-Year Plan” period, China needs to put into operation more than 20 GW of wind power annually. This means that the targets and tasks of wind power development are basically clear, and the wind power industry will maintain a rapid growth for a long period of time. Concerning the benefits of wind power, a prediction system installed in grid-connected wind farms becomes important to effectively reduce the volatility of the voltage and frequency caused by a sudden cut of wind turbines, and to improve the security, reliability, and controllability of an electric power system to realize the economic dispatch. In this sense, an accurate forecast of wind speed is an essential prerequisite, which helps guarantee the construction and operation of the wind power prediction system.

The commonly used methods in terms of wind speed prediction are mainly divided into two categories: statistical analysis models, such as autoregressive moving average (ARMA) models [5] and autoregressive integrated moving average (ARIMA) models [6–8]; and machine learning methods, including artificial neural networks (ANNs) [9–12] and the support vector machine (SVM) [13,14].

Weron [15] explained the complexity of the available solutions, their strengths and weaknesses, and the opportunities and threats that the forecasting tools offer or that may be encountered. Cincotti, et al. [16] proposed and compared three different methods to model prices time series. Amjady and Keynia [17] applied an improved neural network to day-ahead electricity price forecasting. Here, the back propagation neural network (BPNN) is a typical instance of an ANN. Guo [18] introduced a new strategy based on seasonal exponential adjustment and a BPNN to forecast wind speed, where the BPNN was established to predict the wind speed. Liu [19] put forward a BPNN model with empirical mode decomposition (EMD) to forecast hourly wind speed. The experiment was repeated 30 times and took the mean value as the final results to avoid randomness, which indicated that the model performed well. However, the BPNN has a problem with many parameters to set, and it is easy to fall into over-fitting or a local optimum. Compared with a BPNN, the radial basis function neural network (RBFNN) shows a stronger approximation and anti-interference capability with a simple structure. Zhang [20] exploited a novel method based on the wavelet transform (WT) and an RBFNN with the consideration of seasonal factors. The general regression neural network (GRNN) has strong non-linear mapping capabilities and a flexible network structure as well as a high degree of fault tolerance and robustness, which is suitable for solving nonlinear problems. Moreover, it has more advantages than the RBFNN in approach ability and learning speed. Liu [21] proposed a GRNN model on the basis of an integration of a WT and spectral clustering (SC), which presented a high operation efficiency and prediction accuracy. Thus, a GRNN is considered as the forecasting model in this paper.

The selection of the smoothing factor in the GRNN model has an influence on its performance. Intelligent optimization algorithms, such as the genetic algorithm (GA) [22–24] and particle swarm optimization (PSO) [25–28], are usually taken to select the parameters for forecasting models. PSO is designed by simulating the feeding behavior of birds. Assuming that there is only one piece of food in the area (that is, the optimal solution in question), the task of the flock is to find the food source. During the entire search process, members of the flock pass on their own messages to each other so that other birds know their place. Through such collaborations, they can determine whether they are finding the optimal solution or not and at the same time pass the information of the optimal solution to the entire flock. Eventually, the whole flock can gather around the food source, which means that the optimal solution is found. Ren [29] developed an improved PSO-BPNN model with input parameter selection for wind speed prediction. The study showed that the model optimized by PSO had better results than a single BPNN and an ARIMA model. The PSO effectively improved the forecasting accuracy but also showed the malpractice that, under the condition of convergence, since all the particles fly towards the direction of the optimal solution, the particles tend to be the same, which makes the convergence speed of the latter part slow down significantly. Meanwhile, PSO converges to a certain precision, and cannot be further optimized, thus the accuracy is not high. In order to overcome these drawbacks, the fruit fly optimization algorithm (FOA) based on the behaviors of food finding was proposed by Pan in 2011 [30]. This method needs to set less parameters, performs at a relatively high speed for searching for the optimum, and has a wide application [31–33]. Here, the FOA is utilized to adjust the appropriate smoothing factor in the GRNN model.

The strong randomness and volatility of wind speed add difficulties to its accurate prediction, therefore its inherent characteristics must be taken into account. The original wind speed series can be regarded as a combination of sub-series with different frequency which show more regularities. EMD [34,35] decomposes the signal according to the time-scale characteristics of the data itself without any pre-setting basis function, which is essentially different from the Fourier decomposition and wavelet decomposition methods that are based on the priori harmonic basis functions and wavelet basis functions. Precisely because of this characteristic, EMD can theoretically be applied to any type of signal decomposition and has very obvious advantages for processing nonstationary and nonlinear data. In reference [36], an ANN model integrated with EMD was proposed, where EMD was utilized to decompose the original wind speed series to eliminate its irregular fluctuations. Wang [37] hybridized an Elman Neural Network (ENN) method with EMD. The results showed that it indicated a higher

prediction accuracy than the single ENN model. Therefore, EMD is applied to decompose the original datasets in this study.

According to the above research, a GRNN model integrated with EMD and FOA is proposed. It is the first time that these three models have been combined in wind speed forecasting, and several comparing methods are utilized to validate the effectiveness of the proposed hybrid model. The paper is organized as follows. Section 2 introduces the implementation process of EMD and the GRNN optimized using the FOA. Section 3 presents the evaluation criteria of the results. Section 4 provides a case to validate the proposed model. Section 5 analyzes another case in a different place at another time to prove the generalization of the forecasting method. Section 6 obtains the conclusion in this paper.

## 2. Methodology

### 2.1. EMD

EMD is an adaptive time series decomposition technique proposed by Norden E. Huang [38]. The principle of this signal processing method is to decompose the original time series with various fluctuations into a stationary one with different characteristics. Each series that is obtained after decomposition is treated as an intrinsic mode function (IMF), which satisfies the following two conditions: (1) in the whole time range, the number of local extremal points and over zero must be equal, or the maximum difference is one; and (2) the mean value of the two envelopes formed by the local maxima and local minima, respectively, is zero at any point.

For the original time series  $s(t)$ , the procedures of EMD are shown as follows:

- (1) Apply cubic spline interpolation to connect all the local maxima and minima after identification in the time series  $s(t)$  so that the upper envelope  $x_{\max}(t)$  and lower envelope  $x_{\min}(t)$  are accordingly formed. Calculate the mean value  $n(t)$  of the two envelopes and the difference between  $n(t)$  and the original signal  $s(t)$ :

$$n(t) = \frac{x_{\max}(t) + x_{\min}(t)}{2} \quad (1)$$

$$p(t) = s(t) - n(t) \quad (2)$$

- (2) Identify whether  $p(t)$  satisfies the two conditions of IMFs. If it conforms,  $p(t)$  can be considered as the first IMF; then, calculate the difference between the original signal  $s(t)$  and  $c_1(t)$ :

$$c_1(t) = p(t) \quad (3)$$

$$r_1(t) = s(t) - c_1(t) \quad (4)$$

If not, repeat the above procedure until it meets the two conditions.

- (3) The sifting process above will be repeated  $n$  times until  $r_n$  is a monotone function. The original signal  $s(t)$  can be reconstructed as follows:

$$s(t) = \sum_{i=1}^n c_i + r_n \quad (5)$$

where  $c_i$  represents the IMFs, and  $r_n$  is the final residue.

### 2.2. GRNN

The GRNN model was proposed by the American scholar Donald F. Specht in 1991 [39]. The GRNN model has strong nonlinear mapping capabilities and flexible network structure as well as a high degree of fault tolerance and robustness, which is suitable for solving nonlinear problems. Moreover, it has more advantages than an RBFNN in approach ability and learning speed. The GRNN model is structurally similar to an RBFNN. It consists of four layers, as shown in Figure 1, which are

the input layer, the pattern layer, the summation layer, and the output layer. Corresponding to the network input is  $\mathbf{X} = [X_1, X_2, \dots, X_n]^T$ , and its output is  $\mathbf{Y} = [Y_1, Y_2, \dots, Y_k]^T$ .

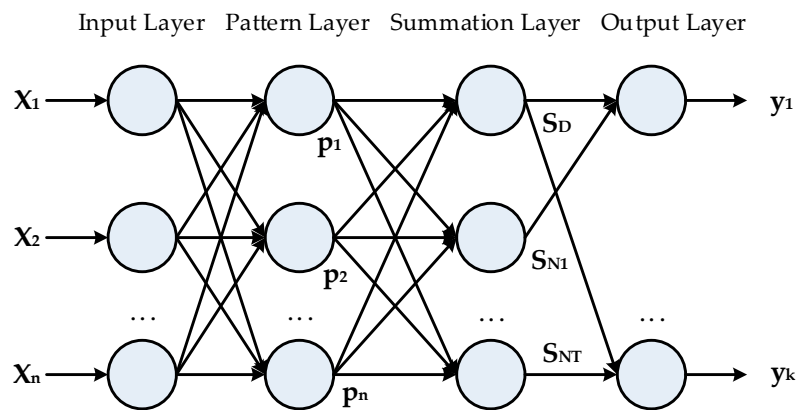


**Figure 1.** The structure of the general regression neural network (GRNN).

- (1) input layer. The number of neurons is equal to the dimension of the input vector in the learning sample. Each neuron is a simple distribution unit that passes the input variable directly to the pattern layer.
- (2) pattern layer. The number of neurons is equal to the number of learning samples. Each neuron corresponds to a different sample, and the neuron transfer function is:

$$p_i = \exp \left[ -\frac{(\mathbf{X} - \mathbf{X}_i)^T (\mathbf{X} - \mathbf{X}_i)}{2\sigma^2} \right], \quad i = 1, 2, \dots, n \quad (6)$$

where  $\mathbf{X}$  represents the network input variable,  $\mathbf{X}_i$  is the corresponding learning sample of neuron  $i$ , and  $\sigma$  belongs to the width coefficient of the Gaussian function, which is called the smoothing factor.

- (3) summation layer. Two types of neurons are used for summation.

One kind of calculation formula is  $\sum_{i=1}^n \exp \left[ -\frac{(\mathbf{X} - \mathbf{X}_i)^T (\mathbf{X} - \mathbf{X}_i)}{2\sigma^2} \right]$ , which sums up the output of all neurons in pattern layer, and the connection weight between the pattern layer and each neuron equals 1. The transfer function is

$$S_D = \sum_{i=1}^n P_i \quad (7)$$

Another calculation formula is  $\sum_{i=1}^n Y_i \exp \left[ -\frac{(\mathbf{X} - \mathbf{X}_i)^T (\mathbf{X} - \mathbf{X}_i)}{2\sigma^2} \right]$ , which performs weighted summation on all the neurons in the pattern layer. The connection weight between the  $i$ th neuron in the pattern layer and the  $j$ th molecule in the summation layer is the  $j$ th element of  $i$ th output sample  $Y_i$ . The transfer function is

$$S_{Nj} = \sum_{i=1}^n y_{ij} P_i, \quad j = 1, 2, \dots, k \quad (8)$$

- (4) output layer. The number of neurons is equal to the dimension  $k$  of the output vector in the sample. Each neuron will divide the output of the summation layer, and the output of neuron  $j$  corresponds to the  $j$ th element of the estimated result  $\hat{Y}(\mathbf{X})$ , namely

$$y_j = \frac{S_{Nj}}{S_D}, \quad j = 1, 2, \dots, k \quad (9)$$

When the smooth factor  $\sigma$  is very large,  $\hat{Y}(X)$  is approximately the mean of all the sample-dependent variables. On the contrary, when the smooth factor tends to 0,  $\hat{Y}(X)$  is very close to the training sample. When the point to be predicted is included in the training sample set, the forecasting value of the dependent variable will be very close to the corresponding dependent variable in the sample. Once encountered, the sample cannot be included in the point, and it is possible to predict a very poor performance, which indicates that the network has a poor generalization ability. When the value of  $\sigma$  is moderate, the dependent variable of all of the training samples is considered in the estimation  $\hat{Y}(X)$ , and the dependent variable corresponding to the forecasting point distance is added to the larger weight. Therefore, the value of  $\sigma$  has a great influence on the forecasting results of the GRNN, and the FOA is used to find the optimal processing of  $\sigma$ .

### 2.3. A GRNN Based on the FOA with Parameter Selection

The FOA is a new global optimization method based on foraging behaviors. The fruit flies themselves are superior in smell and vision to other species; specifically, they can collect all kinds of smells in the air and fly in the direction of the food or gather with companions. Thus, there are two steps for searching for food of a fruit fly swarm [30]: (1) use an olfactory organ to collect odors floating in the air and fly towards the food location; and (2) use vision to find food and other fruit flies' gathering position and fly to that direction. The iterative food searching process of a fruit fly swarm is shown in Figure 2. Compared with PSO, the FOA has strong robustness as a result of the algorithm's operation not involving multiple loops and complicated functions. An optimization problem with only one parameter can achieve very good results. In this paper, the FOA is utilized to select the best value of the smoothing factor  $\sigma$  in the GRNN.

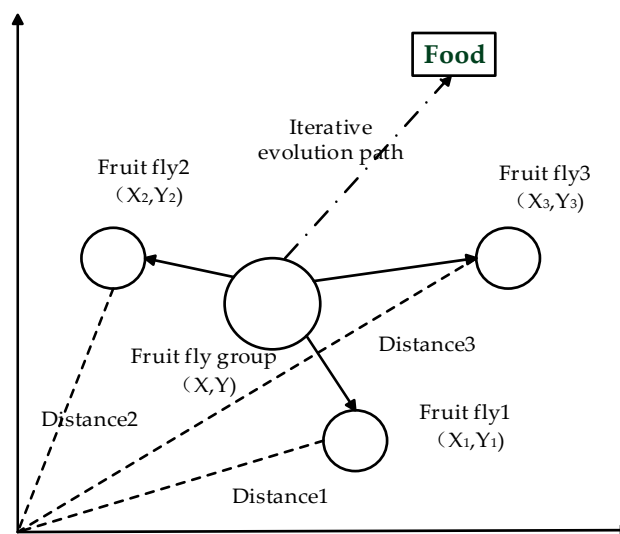


**Figure 2.** Iterative food searching process of a fruit fly swarm.

The wind speed forecasting model combining EMD, the FOA, and the GRNN are constructed as illustrated in Figure 3.

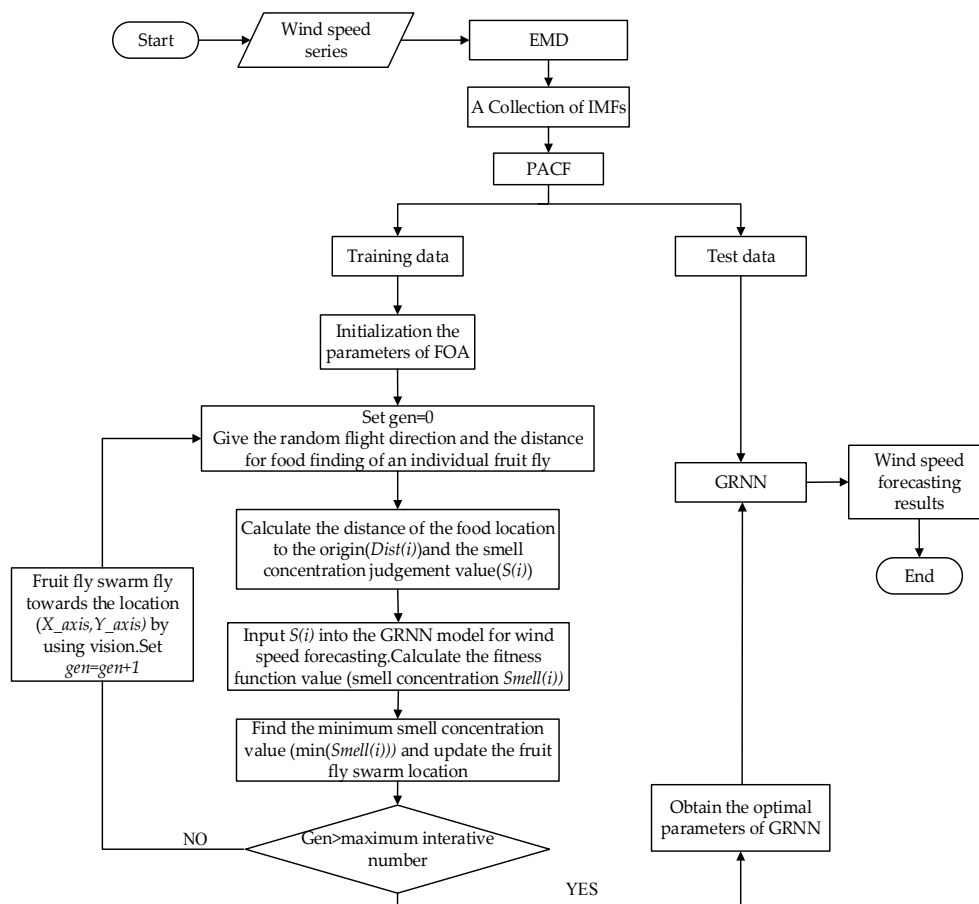


**Figure 3.** The flow chart of EMD-FOA-GRNN. EMD: empirical mode decomposition; IMF: intrinsic mode function; PACF: partial autocorrelation coefficient function; FOA: fruit fly optimization algorithm.

The specific steps for wind speed prediction are listed as follows:

Step 1: Decompose the original wind series into a collection of IMFs by EMD. In order to choose a proper input, the partial autocorrelation coefficient function (PACF) is applied to each of the IMFs to select the elements for the training set. For the stationary time series  $\{Y_t\}$ , the so-called k-order lag PACF refers to the correlation between  $y_{t-k}$  and  $y_t$  under the condition of a given middle random variable  $y_{t-1}, y_{t-2}, \dots, y_{t-k+1}$ , or after eliminating the interference of the middle random variable  $y_{t-1}, y_{t-2}, \dots, y_{t-k+1}$ .

Step 2: Initialize the parameters: after many attempts, the optimal population size and the maximum iteration number are respectively proposed as 20 and 50. The initial position of the fruit fly swarm is set as  $X\_axis = rand(), Y\_axis = rand()$ , where  $rand()$  represents the random number generation function. Here, according to general value range of the smoothing factor  $\sigma$ , the range of random flight distance is set as  $(-10, 10)$ . To avoid overtraining, the samples are divided into two groups to carry out the cross-training.

Step 3: Start searching for the optimum: according to the operation mechanism of the FOA [29], set the number of iterations  $gen = 0$ , and let  $[X(i), Y(i)]$  be the random direction and distance that an individual fruit fly follows to look for food.

$$X(i) = X\_axis + 20 \times rand() - 10 \quad (10)$$

$$Y(i) = Y\_axis + 20 \times rand() - 10 \quad (11)$$

Step 4: Evaluate the population: firstly, calculate the distance  $Dist(i)$  from the location of the fruit fly to the origin and take the reciprocal of  $Dist(i)$  as the smell concentration judgment value  $S(i)$ .

$$Dist(i) = \left( X(i)^2 + Y(i)^2 \right)^{\frac{1}{2}} \quad (12)$$

$$S(i) = \frac{1}{Dist(i)} \quad (13)$$

Secondly, set  $S(i)$  as the value of the smoothing factor in the GRNN to predict the wind speed. Thirdly, select the root mean square error as the fitness function ( $Function()$ ) to evaluate the disparity between the actual value and forecasting result, and record the corresponding value as the smell concentration  $Smell(i)$ . Finally, the fruit fly with the minimal smell concentration can be found out.

$$Smell(i) = Function(S(i)) \quad (14)$$

$$\left[ \begin{array}{cc} bestSmell & bestIndex \end{array} \right] = \min(Smell(i)) \quad (15)$$

Step 5: Record the optimal value. The best smell concentration value  $Smellbest$ , smell concentration judgment  $bestS(i)$ , and the  $x$  and  $y$  coordinates need to be kept as follows. Then, the fruit flies utilize vision to fly towards that location.

$$Smellbest = bestSmell \quad (16)$$

$$bestS(i) = S(bestIndex) \quad (17)$$

$$X\_axis = X(bestIndex) \quad (18)$$

$$Y\_axis = Y(bestIndex) \quad (19)$$

Step 6: Implement iteration optimization. Repeat Step 3 and Step 4 to determine whether the smell concentration is better than the previous one. If it is, go to Step 5 and set  $gen = gen + 1$ .

Step 7: Stop optimization and start prediction. Circulation ends at the maximum number of iterations. Here, the best value of the smoothing factor can be substituted into the GRNN model for wind speed forecasting.

### 3. Evaluation Criteria of Forecasting Performance

It is the primary issue to determine which forecasting model outperforms the other models, and the performance of the prediction models is usually assessed by statistical criteria: the mean absolute error (MAE), the mean absolute percentage error (MAPE), the root mean square error (RMSE), and the index of agreement (IoA). For the first three indexes, the smaller the values are, the better the forecasting performance is. For the IoA, the closer the value is to 1, the better the forecasting performance is. In addition, an  $MAPE < 10\%$  indicates high prediction accuracy,  $10\% \leq MAPE \leq 20\%$  indicates good prediction,  $20\% \leq MAPE \leq 50\%$  implies acceptable prediction, and an  $MAPE \geq 50\%$  implies inaccurate prediction [9]. These four error indexes are defined as follows:

$$MAE = \frac{1}{N} \sum_{t=1}^N |y_t - y_t^*| \quad (20)$$

$$MAPE = \frac{1}{N} \sum_{t=1}^N \left| \frac{y_t - y_t^*}{y_t} \right| \times 100\% \quad (21)$$

$$RMSE = \sqrt{\frac{1}{N} \sum_{t=1}^N (y_t - y_t^*)^2} \quad (22)$$

$$\text{IoA} = 1 - \frac{\sum_{t=1}^N (y_t^* - y_t)^2}{\sum_{t=1}^N (|y_t^* - \bar{y}_t| - |y_t - \bar{y}_t|)^2} \quad (23)$$

where  $y_t$  and  $y_t^*$  are the actual and forecast wind speeds at time period  $t$ , respectively;  $N$  is the forecasting period; and  $\bar{y}_t$  represents the mean value of the actual wind speed at time period  $t$ .

Additionally, in order to show the improvement degree of forecasting errors for different models,  $\xi$  is defined as follows:

$$\xi = \begin{cases} \frac{\zeta^{\text{compared}} - \zeta^{\text{proposed}}}{\zeta^{\text{compared}}} \times 100\% & \text{suitable for MAE, MAPE and RMSE} \\ \frac{\zeta^{\text{proposed}} - \zeta^{\text{compared}}}{\zeta^{\text{compared}}} \times 100\% & \text{suitable for IoA} \end{cases} \quad (24)$$

where  $\zeta^{\text{proposed}}$  and  $\zeta^{\text{compared}}$  represent the MAE, MAPE, RMSE, and IoA generated by the proposed model and other compared models, respectively.

## 4. Case Study

### 4.1. Wind Speed Data

Gansu province, with a wealth of wind energy resources, is one of the top seven 10-million-kilowatt wind power bases heavily invested for construction in China. Located in Jiuquan City, Guazhou is known as “the World Storehouse of Wind Energy”, whose geographical position is shown in Figure 4. In recent years, a series of favorable policies have been issued to promote the further development of wind power generation in this area. The installed wind capacity is expected to reach 6.45 million kW and the annual generating capacity will come to 14 billion kWh in 2015 for the Guazhou region. According to preliminary planning, by 2020, the total installed wind capacity will exceed 10 million kW. Therefore, accurate wind speed forecasting is not only the basis for wind power prediction, but also has profound significance for planning and designing a wind farm, making a schedule for operating the generator, ensuring the safe operation of the electric power system, and improving economic benefits, etc.

The wind speed data every 20 min from 28 October 2011 to 1 December 2011 were collected from a wind farm in the northwest of Guazhou, totaling 2520 records. Here, the data from 28 October 2011 to 28 November 2011 are selected as the training set and the remaining 216 data are utilized as the test set. Figure 5 shows the original wind speed time series (including 2304 samplings) with its nonlinear and nonstationary characteristics.



Figure 4. The geographical location of Guazhou Region.

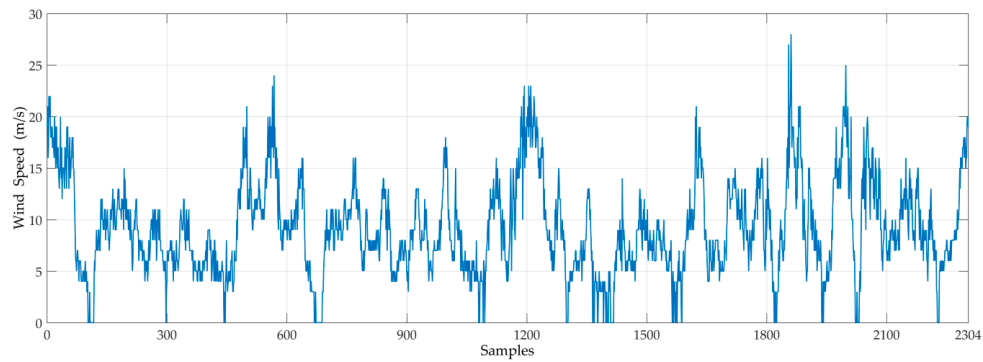


**Figure 5.** Original wind speed series from 28 October 2011 to 28 November 2011.

#### 4.2. Forecasting Steps

Step 1: Wind speed decomposition. EMD is applied to decompose the original wind speed series into several IMFs to eliminate the nonstationarity of the data, which may have an impact on prediction accuracy. From Figure 6, it can be observed that until eight independent IMFs and one residue R0 are decomposed, the wind speed time series in this case satisfies the condition of EMD.

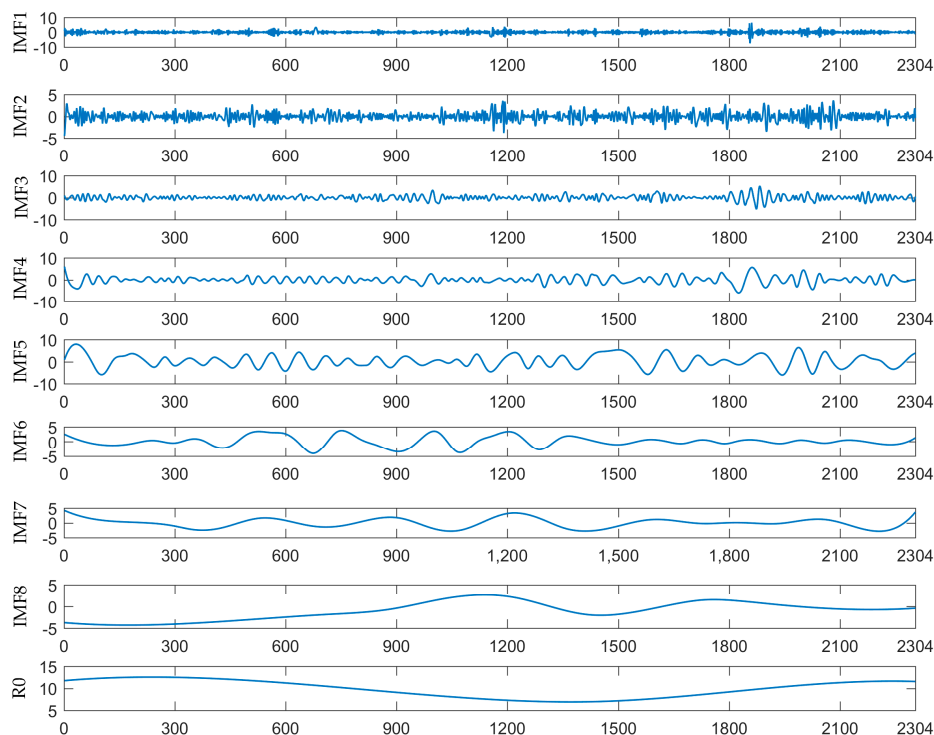


**Figure 6.** The EMD results of original wind speed series.

Step 2: Input variables selection based on PACF. Since the weather variables that may affect wind speed cannot be easily collected, and the wind speed shows certain time series characteristics, the wind speed data values before the forecast wind speed point are considered as the input variables of the GRNN, and the PACF is applied to determine the specific input variable number of each of the IMFs and R0. Figure 7 is the plot of the partial correlation analysis of the wind speed, where PACF1~PACF8 stand for IMFs (PACF1~PACF8), respectively, and PACF9 represents the residue (R0). Setting each decomposition wind speed time series  $x_i$  as the output variable, if the PACF at lag  $k$  is out of the 95% confidence interval,  $x_{i-k}$  is applied as one of the input variables.

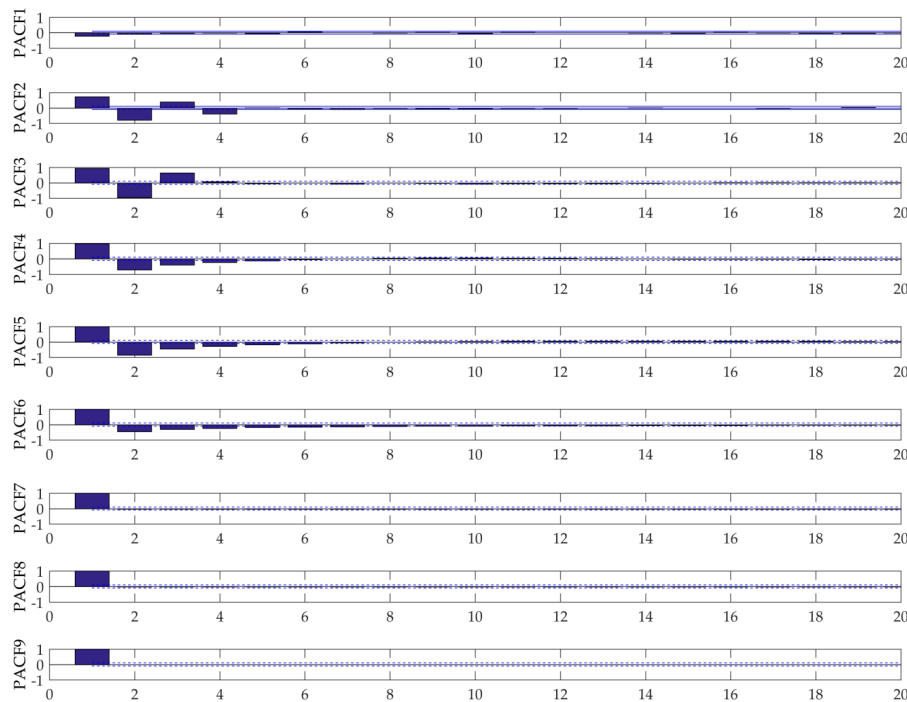


Figure 7. The PACFs of the IMFs and R0.

So, it is obvious that the input variables of these nine series for the FOA-GRNN are the ones shown as follows.

- IMF1:  $(x_{t-1})$
- IMF2:  $(x_{t-1}, x_{t-2}, x_{t-3}, x_{t-4})$
- IMF3:  $(x_{t-1}, x_{t-2}, x_{t-3})$
- IMF4:  $(x_{t-1}, x_{t-2}, x_{t-3}, x_{t-4}, x_{t-5})$
- IMF5:  $(x_{t-1}, x_{t-2}, x_{t-3}, x_{t-4}, x_{t-5}, x_{t-6})$
- IMF6:  $(x_{t-1}, x_{t-2}, x_{t-3}, x_{t-4}, x_{t-5}, x_{t-6}, x_{t-7}, x_{t-8}, x_{t-9})$
- IMF7:  $(x_{t-1})$
- IMF8:  $(x_{t-1})$
- R0:  $(x_{t-1})$

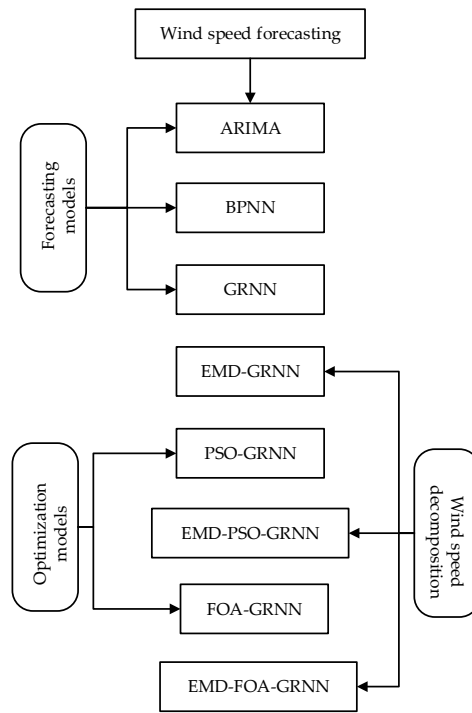
Step 3: Wind speed forecasting. The FOA-GRNN is utilized to predict the corresponding sub-series with the selected input variables in Step 2. The final forecasting results for the wind speed from 29 November 2011 to 1 December 2011 are obtained by aggregating the prediction results of each sub-series. The values of the smoothing factor in the GRNN optimized by the FOA are recorded in Table 1 for these IMFs and R0.

Table 1. The values of the smoothing factor for each FOA-GRNN trained by the IMFs and R0.

IMFs	IMF1	IMF2	IMF3	IMF4	IMF5	IMF6	IMF7	IMF8	R0
Smoothing factor	0.0652	0.0330	0.0076	0.0128	0.0109	0.0273	0.0031	0.0023	0.0023

Step 4: Comparative analysis of different models. From Figure 8, eight models are presented to predict the wind speed. The ARIMA, BPNN, and GRNN models are three different basic forecasting models. Since PSO and the FOA both belong to the class of swarm intelligent optimization algorithms, there are similarities in the operating mechanism. Thus, the PSO-GRNN and the FOA-GRNN are

utilized to test whether the optimization part donates to the prediction accuracy. The EMD-GRNN, the EMD-PSO-GRNN, and the EMD-FOA-GRNN can be applied to explore the effectiveness of EMD. After many attempts, the proper parameters settings in each algorithm are displayed in Table 2. The wind speed actual and forecasting values for different models are shown in Figures 9 and 10.



**Figure 8.** Comparison framework for wind speed forecasting models. ARIMA: autoregressive integrated moving average.

**Table 2.** The parameters settings in each of the comparison models.

Algorithm	Affiliated Comparison Model	Parameter Name	Value Setting
BPNN	BPNN	maximum iteration number	50
		learning rate	0.1
		minimum error	0.001
GRNN	GRNN	smoothing factor	0.05
	PSO-GRNN		
	EMD-GRNN		
	EMD-PSO-GRNN		
PSO	PSO-GRNN EMD-PSO-GRNN	population size	20
		maximum iteration number	50
		learning factor c1, c2	0.8, 0.8
		maximum velocity	1
		minimum error	0.001

BPNN: back propagation neural network; PSO: particle swarm optimization.

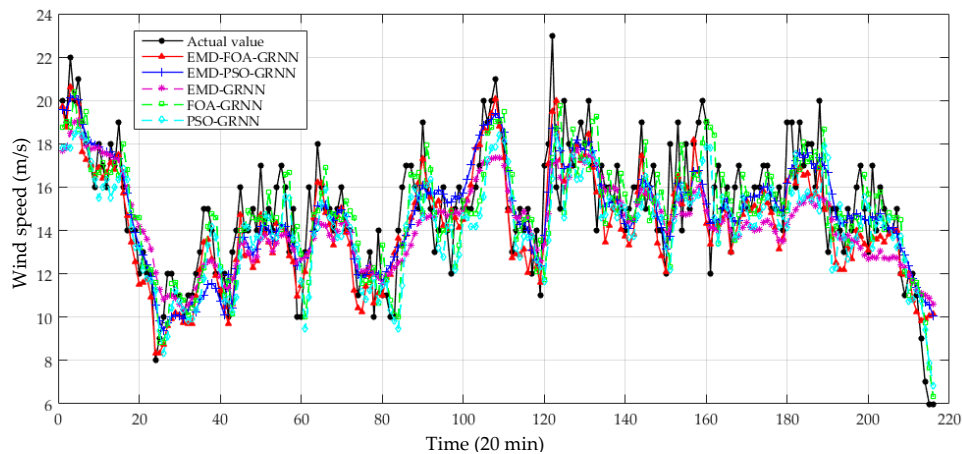


**Figure 9.** Prediction results of wind speed from 29 November 2011 to 1 December 2011 (I).

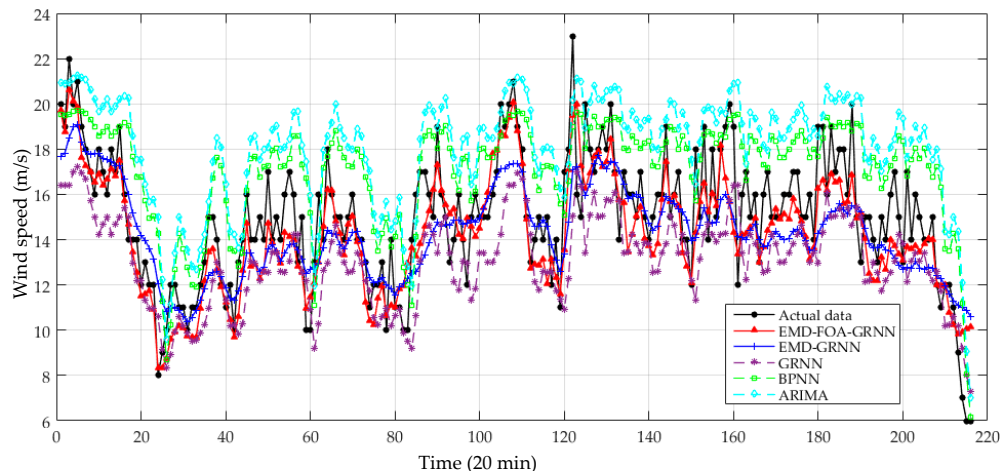
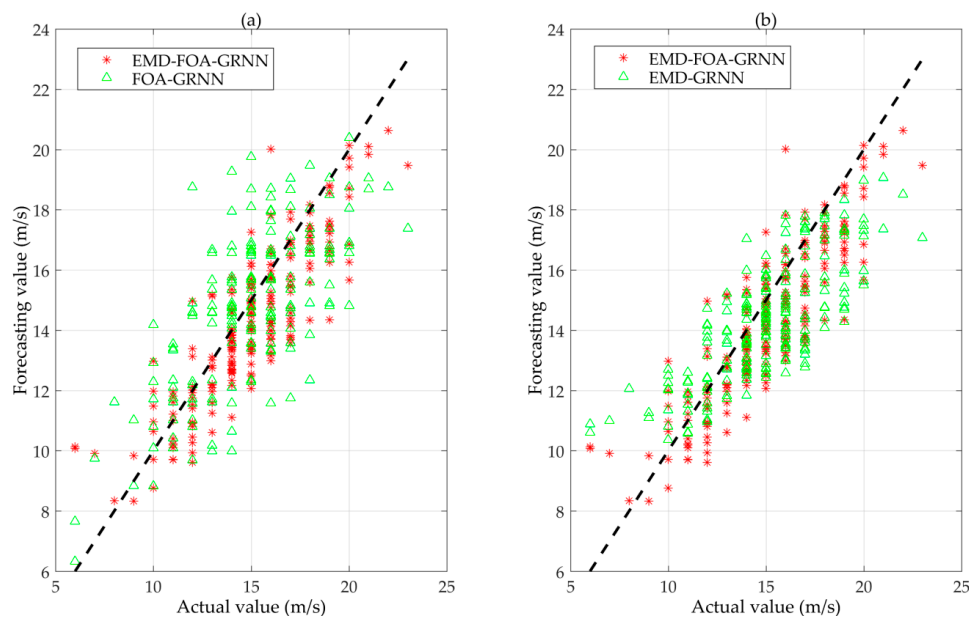


**Figure 10.** Prediction results of wind speed from 29 November 2011 to 1 December 2011 (II).

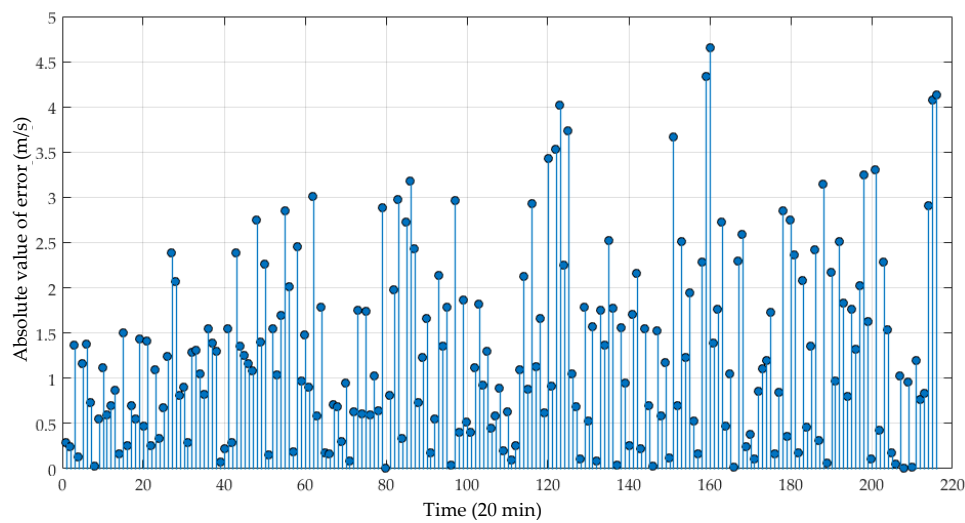
#### 4.3. Results Analysis

Figure 11 displays the degree of correlation between the actual value and predicted values of the wind speed. It can be seen that the forecasted wind speed obtained by the EMD-FOA-GRNN model most correlates to the actual one compared with the FOA-GRNN and EMD-GRNN models.

As is presented in Figure 12, the absolute value of error by the EMD-FOA-GRNN model is relatively stable and there are only five error points out of 4 m/s, which means that the forecasting results can be accepted. The accuracy estimation of the predicted wind speed by different models is shown in Table 3. It can be observed that the relative errors in the hybrid models mainly concentrate on the level of less than 10%. Moreover, the number of errors less than 10% generated by the EMD-FOA-GRNN, EMD-PSO-GRNN, and EMD-GRNN models is more than 120, which shows a good performance in wind speed forecasting.



**Figure 11.** The correlation between forecasting and actual wind speed. (a) EMD-FOA-GRNN and FOA-GRNN; (b) EMD-FOA-GRNN and EMD-GRNN.



**Figure 12.** The absolute value of error by the EMD-FOA-GRNN model.

**Table 3.** Accuracy estimation of forecasting models for the test samples.

Forecasting Models	<10%		10–20%		>20%	
	Number	Percentage	Number	Percentage	Number	Percentage
EMD-FOA-GRNN	140	64.81%	65	30.09%	11	5.09%
EMD-PSO-GRNN	139	64.35%	60	27.78%	17	7.87%
EMD-GRNN	126	58.33%	61	28.24%	29	13.43%
FOA-GRNN	118	54.63%	59	27.31%	39	18.06%
PSO-GRNN	105	48.61%	80	37.04%	31	14.35%
GRNN	80	37.04%	73	33.80%	63	29.17%
BPNN	73	33.80%	57	26.39%	86	39.81%
ARIMA	49	22.69%	55	25.46%	112	51.85%

From Table 4, it can be analyzed that: (a) based on the four evaluation criteria MAE, MAPE, RMSE, and IoA, the proposed model EMD-FOA-GRNN shows the best forecasting performance among the eight models. The MAE, MAPE, RMSE, and IoA of the proposed model is 1.286 m/s, 8.95%, 0.124 m/s, and 0.9070, respectively. (b) by comparing the three single models, the GRNN and the BPNN have higher accuracy than the ARIMA model. Therefore, it can be concluded that intelligent models can obtain better forecasting results than statistical models. Additionally, the GRNN presents more satisfactory performance than the BPNN. The prediction accuracy of the BPNN is closely related to typical training samples and network structure, and it is easy to fall into a local extreme. However, the GRNN, with only one parameter to be optimized, is more suitable for forecasting nonlinear and non-stationary wind speed series. (c) when comparing the EMD-FOA-GRNN with the FOA-GRNN, the EMD-PSO-GRNN with the PSO-GRNN, and the EMD-GRNN with the GRNN, EMD improves the forecasting performance in terms of lower MAE, MAPE, RMSE, and a higher IoA, which proves it can effectively decompose the volatile signals to promote the forecasting capacity. (d) the two optimized models PSO-GRNN and FOA-GRNN produce better results than the single GRNN model. Here, the FOA and the PSO algorithm are utilized to select the appropriate value of the smoothing factor for the GRNN. These two optimization algorithms can effectively enhance the training and learning process so as to avoid falling into a local optimum and improve the global searching ability of the GRNN. Moreover, as seen from these four indexes' values, the FOA made a better optimal performance than that of PSO, which verified the optimization mechanism of the FOA.

**Table 4.** Statistical error measures of prediction methods in Case One.

Forecasting Models	Indexes			
	MAE (m/s)	MAPE (%)	RMSE (m/s)	IoA
EMD-FOA-GRNN	1.286	8.95	0.124	0.9070
EMD-PSO-GRNN	1.320	9.45	0.135	0.8921
EMD-GRNN	1.593	10.99	0.151	0.8195
FOA-GRNN	1.657	11.38	0.146	0.8354
PSO-GRNN	1.739	11.57	0.145	0.8124
GRNN	2.265	14.50	0.171	0.7310
BPNN	2.461	18.26	0.231	0.7257
ARIMA	3.197	23.52	0.285	0.6618

MAE: mean absolute error; MAPE: mean absolute percentage error; RMSE: root mean square error; IoA: Index of Agreement.

From Table 5, it can be found that: (a) the forecasting performance of the EMD-GRNN combined with the PSO algorithm and the FOA have been effectively improved. It can be seen that the FOA performs better than the PSO algorithm in improving prediction accuracy, mainly because it is easier to use the FOA to fulfill a global optimization goal with less parameters to be optimized. (b) For the basic EMD-GRNN model, it can be analyzed that the FOA enhances the forecasting accuracy and the MAPE promoted percentage is 18.56%. Similarly, owing to EMD, the promoted percentage of MAPE is 21.35%. (c) The EMD part makes more of a contribution than the FOA part in the EMD-FOA-GRNN model.

**Table 5.** Promoted percentage of errors in Case One.

Forecasting Models	Promoted Percentage of Errors (%)			
	$\zeta_{MAE}$	$\zeta_{MAPE}$	$\zeta_{RMSE}$	$\zeta_{IoA}$
EMD-FOA-GRNN versus EMD-GRNN	19.27	18.56	17.88	10.68
EMD-FOA-GRNN versus FOA-GRNN	22.39	21.35	15.07	8.57
EMD-PSO-GRNN versus EMD-GRNN	17.14	14.01	10.60	8.86
EMD-PSO-GRNN versus PSO-GRNN	24.09	18.32	6.90	9.81

### 5. Case Two

In order to verify that the proposed model has good adaptability in different times and places, another case which selects the wind speed data in a wind farm located in the middle of Inner Mongolia (shown in Figure 13) is provided in this paper. The study is carried out with the data from 18 February 2012 to 22 March 2012 as the training set and data from 23 March 2012 to 25 March 2012 as the test set. The forecasting results are displayed in Figures 14 and 15. The error analyses are shown in Tables 5 and 6.

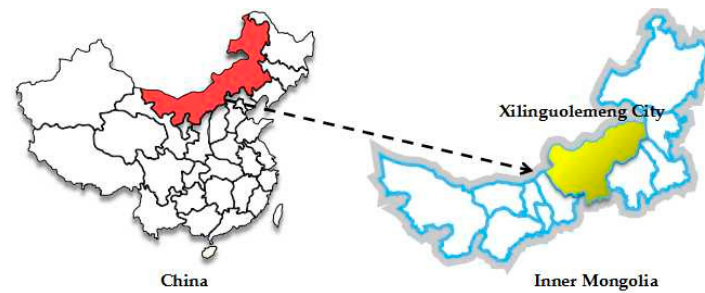


Figure 13. The geographical location of Xilinguolemeng City.

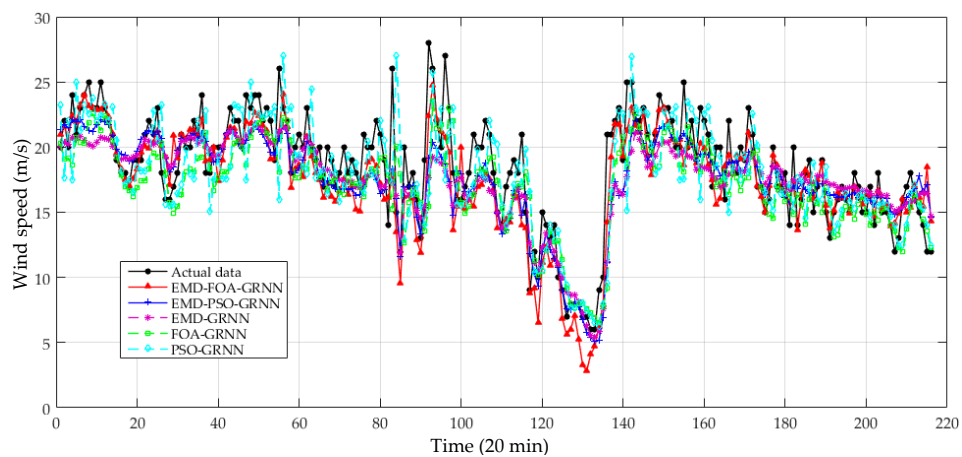


Figure 14. Prediction results of wind speed from 23 March 2012 to 25 March 2012 (III).

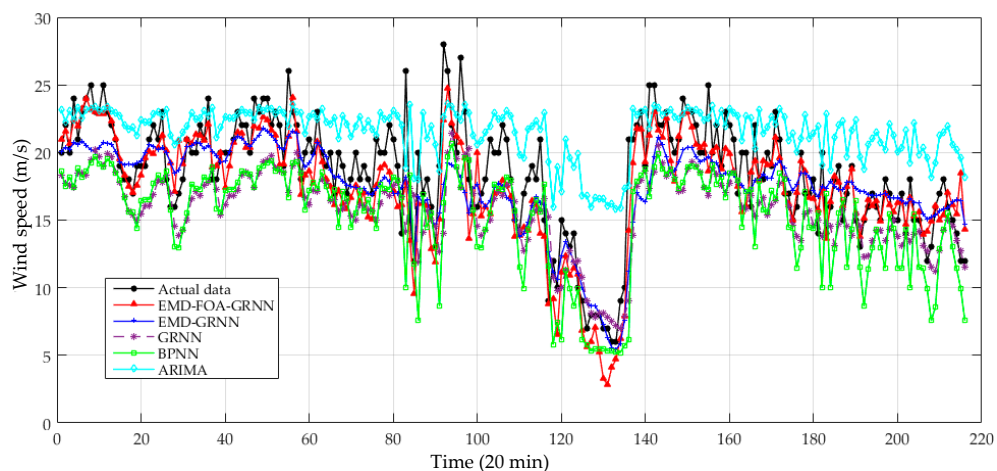


Figure 15. Prediction results of wind speed from 23 March 2012 to 25 March 2012 (IV).

**Table 6.** Statistical error measures of prediction methods in Case Two.

Forecasting Models	Indexes			
	MAE (m/s)	MAPE (%)	RMSE (m/s)	IoA
EMD-FOA-GRNN	1.677	9.87	0.137	0.9288
EMD-PSO-GRNN	1.880	10.16	0.142	0.8941
EMD-GRNN	2.037	10.91	0.147	0.8671
FOA-GRNN	2.300	12.47	0.164	0.8334
PSO-GRNN	2.459	13.53	0.183	0.8264
GRNN	3.164	16.38	0.194	0.7453
BPNN	3.505	18.85	0.226	0.7518
ARIMA	3.594	25.19	0.382	0.6258

As demonstrated in Tables 6 and 7: (a) intelligent algorithms have higher accuracy in wind speed forecasting than statistical models. (b) the hybrid models show better performance than the single one. (c) EMD improves the performance compared with the corresponding forecasting models that directly utilize the original wind speed series to make predictions. (d) The EMD-FOA-GRNN presents the best forecasting results among the models, and the EMD part donates much more than the FOA part in improving prediction precision. In all, the results in Case Two once again verify the feasibility and effectiveness of the proposed model.

**Table 7.** Promoted percentage of errors in Case Two.

Forecasting Models	Promoted Percentage of Errors (%)			
	$\zeta_{MAE}$	$\zeta_{MAPE}$	$\zeta_{RMSE}$	$\zeta_{IoA}$
EMD-FOA-GRNN vs. EMD-GRNN	19.27	18.56	17.88	10.68
EMD-FOA-GRNN vs. FOA-GRNN	22.39	21.35	15.07	8.57
EMD-PSO-GRNN vs. EMD-GRNN	17.14	14.01	10.60	8.86
EMD-PSO-GRNN vs. PSO-GRNN	24.09	18.32	6.90	9.81

## 6. Conclusions

This paper presents a hybrid intelligent algorithm for wind speed forecasting. Firstly, EMD is proposed to preprocess the original wind speed signals to eliminate the random fluctuations of the wind speed data. Then, the GRNN model, which is improved by the FOA, is used to forecast the set of IMFs obtained by EMD. The PACF is used to select the arguments of the GRNN and choose the lags of the historical speeds. Major conclusions are summarized as follows: (a) the EMD effectively improves the forecasting performance; (b) the optimization algorithms FOA and PSO increase the strong global searching capability of the model, and the FOA shows better performance; (c) the EMD part contributes more than the FOA in increasing the accuracy of the EMD-FOA-GRNN model; and (d) the error valuation criteria shows that the EMD-FOA-GRNN is a very promising methodology, which can provide a new idea for short-term wind speed forecasting. In addition, with the development of signal processes and intelligent algorithms, there will be more advanced models applied to predict wind speed, which is our study direction in the future.

**Acknowledgments:** This work is supported by the Natural Science Foundation of China (Project No. 71471059) and the Fundamental Research Funds for the Central Universities (Project No. 2017XS103). Wei-Chiang Hong thanks the research grant sponsored by the Ministry of Science & Technology, Taiwan (MOST 106-2221-E-161-005-MY2).

**Author Contributions:** Yi Liang designed this research and wrote this paper; Dongxiao Niu and Wei-Chiang Hong provided professional guidance.

**Conflicts of Interest:** The authors declare no conflict of interest.

## References

1. Hu, Q.; Zhang, R.; Zhou, Y. Transfer learning for short-term wind speed prediction with deep neural networks. *Renew. Energy* **2016**, *85*, 83–95. [CrossRef]
2. Wang, J.; Hu, J. A robust combination approach for short-term wind speed forecasting and analysis—Combination of the ARIMA (Autoregressive Integrated Moving Average), ELM (Extreme Learning Machine), SVM (Support Vector Machine) and LSSVM (Least Square SVM) forecasts using a GPR (Gaussian Process Regression) model. *Energy* **2015**, *93*, 41–56.
3. Sawyer, S.; Fried, L.; Shukla, S.; Qiao, L. *Global Wind Report 2016—Annual Market Update*; Global Wind Energy Council: Brussels, Belgium, 2017.
4. National Development and Reform Commission. *National Climate Change Program (2014–2020)*; National Development and Reform Commission: Beijing, China, 2014. Available online: <http://www.ndrc.gov.cn/zcfb/zcfbtz/201411/W020141104584717807138.pdf> (accessed on 30 November 2017).
5. Erdem, E.; Shi, J. ARMA based approaches for forecasting the tuple of wind speed and direction. *Appl. Energy* **2011**, *88*, 1405–1414. [CrossRef]
6. Liu, H.; Tian, H.Q.; Li, Y.F. Comparison of two new ARIMA-ANN and ARIMA-kalman hybrid methods for wind speed prediction. *Appl. Energy* **2012**, *98*, 415–424. [CrossRef]
7. Hodge, B.M.; Zeiler, A.; Brooks, D.; Blau, G.; Pekny, J.; Reklatis, G. Improved Wind Power Forecasting with ARIMA Models. *Comput. Aided Chem. Eng.* **2011**, *29*, 1789–1793.
8. Wang, J.; Hu, J.; Ma, K.; Zhang, Y. A self-adaptive hybrid approach for wind speed forecasting. *Renew. Energy* **2015**, *78*, 374–385. [CrossRef]
9. Ramasamy, P.; Chandel, S.S.; Yadav, A.K. Wind speed prediction in the mountainous region of India using an artificial neural network model. *Renew. Energy* **2015**, *80*, 338–347. [CrossRef]
10. Hui, L.; Tian, H.Q.; Li, Y.F.; Zhang, L. Comparison of four Adaboost algorithm based artificial neural networks in wind speed predictions. *Energy Convers. Manag.* **2015**, *92*, 67–81.
11. Zjavka, L. Wind speed forecast correction models using polynomial neural networks. *Renew. Energy* **2015**, *83*, 998–1006. [CrossRef]
12. Babu, C.N.; Reddy, B.E. A moving-average filter based hybrid ARIMA-ANN model for forecasting time series data. *Appl. Soft Comput.* **2014**, *23*, 27–38. [CrossRef]
13. Chen, K.; Yu, J. Short-term wind speed prediction using an unscented Kalman filter based state-space support vector regression approach. *Appl. Energy* **2014**, *113*, 690–705. [CrossRef]
14. Zhou, J.; Jing, S.; Gong, L. Fine tuning support vector machines for short-term wind speed forecasting. *Energy Convers. Manag.* **2011**, *52*, 1990–1998. [CrossRef]
15. Weron, R. Electricity price forecasting: A review of the state-of-the-art with a look into the future. *Int. J. Forecast.* **2014**, *30*, 1030–1081. [CrossRef]
16. Cincotti, S.; Gallo, G.; Ponta, L.; Marco, R. Modeling and forecasting of electricity spot-prices: Computational intelligence vs classical econometrics. *AI Commun.* **2014**, *27*, 301–314.
17. Amjady, N.; Keynia, F. Day ahead price forecasting of electricity markets by a mixed data model and hybrid forecast method. *Int. J. Electr. Power Energy Syst.* **2008**, *30*, 533–546. [CrossRef]
18. Guo, Z.H.; Wu, J.; Lu, H.Y.; Wang, J.Z. A case study on a hybrid wind speed forecasting method using BP neural network. *Knowl.-Based Syst.* **2011**, *24*, 1048–1056. [CrossRef]
19. Liu, H.; Chen, C.; Tian, H.Q.; Li, Y.F. A hybrid model for wind speed prediction using empirical mode decomposition and artificial neural networks. *Renew. Energy* **2012**, *48*, 545–556. [CrossRef]
20. Zhang, W.; Wang, J.; Wang, J.; Zhao, Z.; Tian, M. Short-term wind speed forecasting based on a hybrid model. *Appl. Soft Comput.* **2013**, *13*, 3225–3233. [CrossRef]
21. Liu, D.; Wang, J.; Wang, H. Short-term wind speed forecasting based on spectral clustering and optimized echo state networks. *Renew. Energy* **2015**, *78*, 599–608. [CrossRef]
22. Liu, H.; Tian, H.; Liang, X.; Li, Y. New wind speed forecasting approaches using fast ensemble empirical model decomposition, genetic algorithm, Mind Evolutionary Algorithm and Artificial Neural Networks. *Renew. Energy* **2015**, *83*, 1066–1075. [CrossRef]
23. Liu, H.; Tian, H.Q.; Chen, C.; Li, Y.F. An experimental investigation of two Wavelet-MLP hybrid frameworks for wind speed prediction using GA and PSO optimization. *Int. J. Electr. Power Energy Syst.* **2013**, *52*, 161–173. [CrossRef]

24. Liu, D.; Niu, D.; Wang, H.; Fan, L. Short-term wind speed forecasting using wavelet transform and support vector machines optimized by genetic algorithm. *Renew. Energy* **2014**, *62*, 592–597. [[CrossRef](#)]
25. Yu, S.; Ke, W.; Wei, Y.M. A hybrid self-adaptive Particle Swarm Optimization–Genetic Algorithm–Radial Basis Function model for annual electricity demand prediction. *Energy Convers. Manag.* **2015**, *91*, 176–185. [[CrossRef](#)]
26. Rahmani, R.; Yusof, R.; Seyedmahmoudian, M.; Mekhilef, S. Hybrid technique of ant colony and particle swarm optimization for short term wind energy forecasting. *J. Wind Eng. Ind. Aerodyn.* **2013**, *123*, 163–170. [[CrossRef](#)]
27. Bahrami, S.; Hooshmand, R.A.; Parastegari, M. Short term electric load forecasting by wavelet transform and grey model improved by PSO (particle swarm optimization) algorithm. *Energy* **2014**, *72*, 434–442. [[CrossRef](#)]
28. Yeh, W.C.; Yeh, Y.M.; Chang, P.C.; Ke, Y.C.; Chung, V. Forecasting wind power in the Mai Liao Wind Farm based on the multi-layer perceptron artificial neural network model with improved simplified swarm optimization. *Int. J. Electr. Power Energy Syst.* **2014**, *55*, 741–748. [[CrossRef](#)]
29. Ren, C.; An, N.; Wang, J.; Li, L.; Hu, B.; Shang, D. Optimal parameters selection for BP neural network based on particle swarm optimization: A case study of wind speed forecasting. *Knowl.-Based Syst.* **2014**, *56*, 226–239. [[CrossRef](#)]
30. Pan, W.T. A new fruit fly optimization algorithm: Taking the financial distress model as an example. *Knowl.-Based Syst.* **2012**, *26*, 69–74. [[CrossRef](#)]
31. Li, H.Z.; Guo, S.; Li, C.J.; Sun, J.Q. A hybrid annual power load forecasting model based on generalized regression neural network with fruit fly optimization algorithm. *Knowl.-Based Syst.* **2013**, *37*, 378–387. [[CrossRef](#)]
32. Yuan, X.; Liu, Y.; Xiang, Y.; Ye, X. Parameter identification of BIPT system using chaotic-enhanced fruit fly optimization algorithm. *Appl. Math. Comput.* **2015**, *268*, 1267–1281. [[CrossRef](#)]
33. Dai, H.; Liu, A.; Lu, J.; Dai, S.; Wu, X.; Sun, Y. Optimization about the layout of IMUs in large ship based on fruit fly optimization algorithm. *Opt. Int. J. Light Electron Opt.* **2015**, *126*, 490–493. [[CrossRef](#)]
34. Wang, Y.H.; Yeh, C.H.; Young, H.W.V.; Hu, K.; Lo, M.T. On the computational complexity of the empirical mode decomposition algorithm. *Phys. Stat. Mech. Appl.* **2014**, *400*, 159–167. [[CrossRef](#)]
35. Samet, H.; Marzbani, F. Quantizing the deterministic nonlinearity in wind speed time series. *Renew. Sustain. Energy Rev.* **2014**, *39*, 1143–1154. [[CrossRef](#)]
36. Hong, Y.Y.; Yu, T.H.; Liu, C.Y. Hour-Ahead Wind Speed and Power Forecasting Using Empirical Mode Decomposition. *Energies* **2013**, *6*, 6137–6152. [[CrossRef](#)]
37. Wang, J.; Zhang, W.; Li, Y.; Wang, J.; Dang, Z. Forecasting wind speed using empirical mode decomposition and Elman neural network. *Appl. Soft Comput.* **2014**, *23*, 452–459. [[CrossRef](#)]
38. Huang, N.E. The empirical mode decomposition and the Hilbert spectrum for nonlinear and non-stationary time series analysis. *R. Soc. Lond. Proc.* **1998**, *454*, 903–995. [[CrossRef](#)]
39. Specht, D.F. A general regression neural network. *IEEE Trans. Neural Netw.* **1991**, *2*, 568–576. [[CrossRef](#)] [[PubMed](#)]

